LA-UR- 00 - 3 52 9

Title: UTILIZING RESULTS FROM INSAR TO DEVELOP SEISMIC LOCATION BENCHMARKS AND IMPLICATIONS FOR SEISMIC SOURCE STUDIES

Author(s): Michael L. Begnaud
Aaron A. Velasco
Lee K. Steck

Los Alamos
NATIONAL LABORATORY

DISCLAIMER

DISCLAIMER

Portions of this document may be illegible in electronic image products. Images are produced from the best available original document.

UTILIZING RESULTS FROM INSAR TO DEVELOP SEISMIC LOCATION BENCHMARKS AND IMPLICATIONS FOR SEISMIC SOURCE STUDIES

Michael L. Begnaud, Aaron A. Velasco, Lee K. Steck
Los Alamos National Laboratory

ABSTRACT:

Obtaining accurate seismic event locations is one of the most important goals for monitoring detonations of underground nuclear tests. This is a particular challenge at small magnitudes where the number of recording stations may be less than 20. Although many different procedures are being developed to improve seismic location, most procedures suffer from inadequate testing against accurate information about a seismic event. Events with well-defined attributes, such as latitude, longitude, depth, and origin time, are commonly referred to as ground truth (GT). Ground truth comes in many forms and with many different levels of accuracy.

Interferometric Synthetic Aperture Radar (InSAR) can provide independent and accurate information (ground truth) regarding ground surface deformation and/or rupture. Relating surface deformation to seismic events is trivial when events are large and create a significant surface rupture, such as for the $M_w = 7.5$ event that occurred in the remote northern region of the Tibetan plateau in 1997. The event, which was a vertical strike slip event, appeared anomalous in nature due to the lack of large aftershocks and had an associated surface rupture of over 180 km that was identified and modeled using InSAR. The east-west orientation of the fault rupture provides excellent ground truth for latitude, but is of limited use for longitude. However, a secondary rupture occurred 50 km south of the main shock rupture trace that can provide ground truth with accuracy within 5 km.

The smaller, 5-km-long secondary rupture presents a challenge for relating the deformation to a seismic event. The rupture is believed to have a thrust mechanism; the dip of the fault allows for some separation between the secondary rupture trace and its associated event epicenter, although not as much as is currently observed from catalog locations. Few events within the time period of the InSAR analysis are candidates for the secondary rupture. Of these, we have identified six possible secondary rupture events (mb range = 3.7-4.8, with two magnitudes not reported), based on synthetic tests and residual analysis. All of the candidate events are scattered about the main and secondary rupture. A Joint Hypocenter Determination (JHD) approach applied to the aftershocks using global picks was not able to identify the secondary event. We added regional data and used propagation path corrections to reduce scatter and remove the 20-km bias seen in the main shock location. After preliminary analysis using several different velocity models, none of the candidate events proved to relocate on the surface trace of the secondary rupture. However, one event (mb = not reported) moved from a starting distance of ~106 km to a relocated distance of ~28 km from the secondary rupture, the only candidate event to relocate in relative proximity to the secondary rupture.

OBJECTIVE

One of the most important goals for monitoring detonations of underground nuclear tests is obtaining accurate seismic event locations, particularly for small magnitude events where the number of recording stations may be less than 20. Although many different procedures are being developed to improve seismic location, most procedures suffer from inadequate testing against accurate information about a seismic event. Interferometric Synthetic Aperture Radar (InSAR) can provide independent and accurate information (ground truth) regarding ground surface deformation and/or rupture. Identifying the secondary event within the Tibet aftershock sequence would provide a small ground truth event, a valuable calibration point in this region. We can also use the event to validate the regional location methods, velocity models, and empirical calibration approaches being used for CTBT monitoring.

RESEARCH ACCOMPLISHED

The verifiability of a Comprehensive Test-Ban Treaty (CTBT) depends on the ability to effectively monitor small magnitude (< 4) events, which has an implicit goal of locating seismic events within a contiguous area smaller than 1000 km^2. Although many different procedures are being developed to improve seismic location, most procedures suffer from inadequate testing against accurate information about a seismic event. Events with well-defined attributes, such as latitude, longitude, depth, and origin time, are commonly referred to as ground truth (GT). Ground truth comes in many forms and with many different levels of accuracy. Nuclear tests, mining explosions, or specific calibration explosions have all been used to assess event locations. Deployments of seismic instruments to record and locate aftershock sequences can also give a level of accuracy much greater than sparse global networks of stations (Myers and Schultz, 2000).

A large ($M_w = 7.5$) earthquake occurred in a remote region of Tibet, in the northern region of the Tibetan plateau. The event was a vertical strike slip event and appeared anomalous in nature due to the lack of large aftershocks (Velasco et al., 2000). The event had an associated surface rupture that was identified and modeled using Interferometric Synthetic Apeture Radar (InSAR) (Peltzer et al., 1999). InSAR can provide independent and accurate information (ground truth) regarding ground surface deformation and/or rupture. The Tibetan mainshock created a surface rupture of over 180 km in length (Figure 1), and occurred on a previously mapped fault that was determined using SPOT imagery (Tapponnier and Molnar, 1977). Focal mechanisms are shown for the Tibet mainshock event (Velasco et al., 2000) and a 1973 Ms=6.9 event west of the Tibet mainshock (Molnar and Chen, 1983). The east-west orientation of the fault rupture provides excellent ground truth for latitude, but is of limited use for longitude. However, a secondary rupture occurred 50 km south of the mainshock rupture trace (Peltzer et al., 1999), which can provide ground truth with accuracy within 5 km.

Relating surface deformation to seismic events is trivial when events are large and create significant surface rupture, such as the mainshock. However, the smaller secondary rupture presents a challenge. This 5-km long rupture is believed to have a thrust mechanism (Peltzer, G., personal communication), which implies that the earthquake/aftershock that generated it may be near but not necessarily on the surface trace of the fault. Identifying the secondary event within the aftershock sequence would provide a small ground truth event, a valuable calibration point in this region. We can also use the event to validate the regional location methods, velocity models, and empirical calibration approaches being used for CTBT monitoring. Furthermore, InSAR is providing unique insight for anelasticity in the crust, and co-locating an event may reveal unique insight into the rupture. In this paper, we focus on identifying the secondary rupture by adding more regional data, attempting to use S-phases, creating synthetic tests, using various velocity models, and hypothesis testing.

Data and Velocity Models

Figure 1 shows the global USGS event locations prior to the Tibetan mainshock, after the mainshock during a time period in which the InSAR was performed, and until March 1999. There are few events within the time period of the InSAR analysis that are candidates for the secondary rupture. All of the events are scattered and biased south of the rupture, with a 20 km bias for the mainshock location (Steck et al., 2000). A Joint Hypocenter Determination (JHD) approach (Dewey, 1983) applied to the aftershocks using global picks was not able to identify the secondary event (Velasco et al., 2000).

We use the global catalog as a guide to obtain waveform data from the IRIS database for a set of digital seismic stations within 30 degrees of the mainshock. We individually pick regional travel time data for all of the aftershocks of this Tibetan earthquake, pick all regional phases than can be identified (Pn, Pg, Sn, Lg), and explore
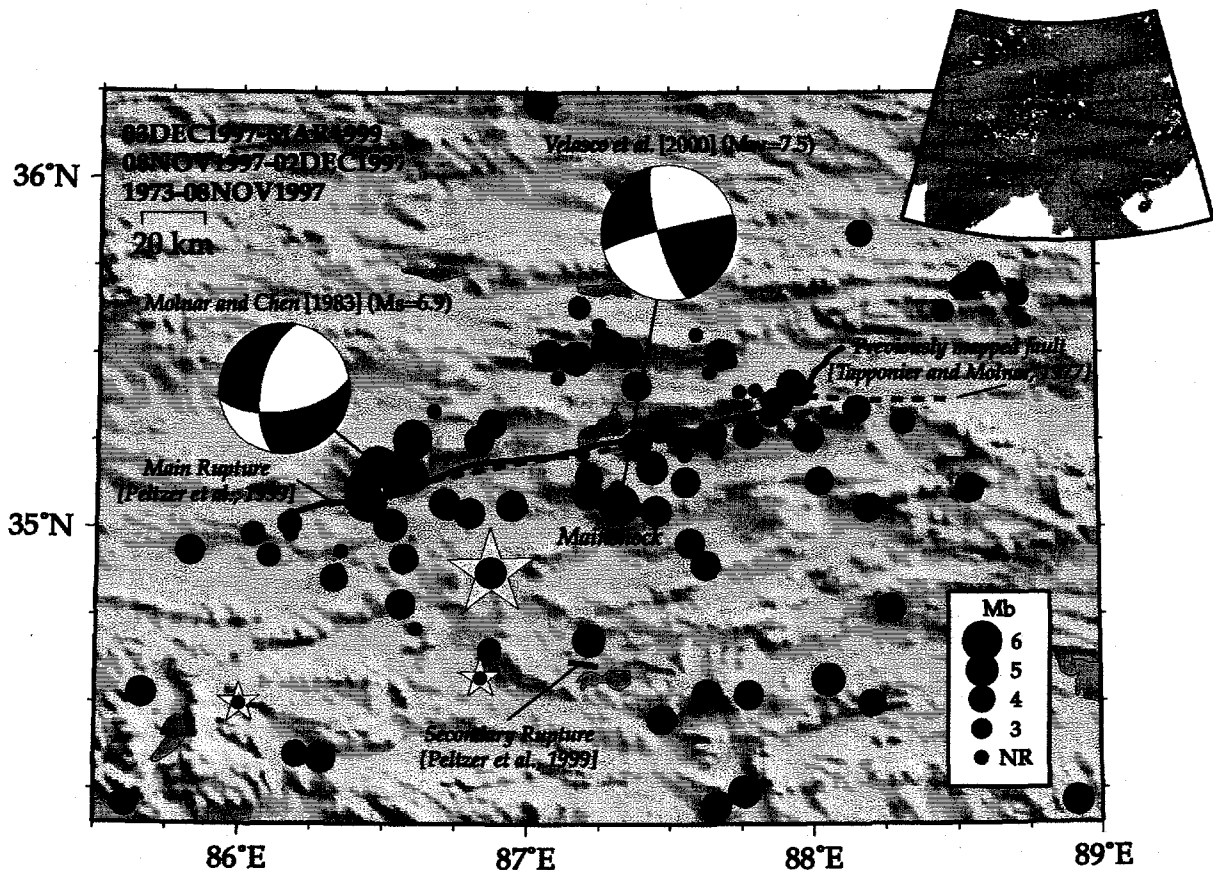
Figure 1. USGS catalog locations for the area around the Manyi/Tibet earthquake (Mw=7.5) on 08NOV1997. Shown are events before and including the mainshock (green), events between the mainshock and the second satellite pass used to create the InSAR image for the center section of the main rupture (red), and events after the second satellite pass through March 1999 (blue). The epicenters between the mainshock and second satellite pass are possible candidates for an event which occurred during the secondary rupture (red line ~50 km south of main rupture), three of which were chosen as the most likely candidates (highlighted). Focal mechanisms are shown for the Manyi mainshock event (Velasco et al., 2000) and a 1973 Ms=6.9 event west of the Manyi mainshock (Molnar and Chen, 1983).

the use of S-phases for location. We merge these regional picks with the global catalog picks from the Reviewed Event Bulletin (REB) developed by the preliminary International Data Center (pIDC) and the United States Geological Survey (USGS) Earthquake Data Reports (EDR).

For the seismic event relocation procedure (described below), two types of errors are used to provide weighting of the arrivals for the inversions: modeling and measurement errors. Measurement error is the error associated with the travel-time picks, and can be estimated using a signal-to-noise ratio (snr) criteria. However, many of the global picks do not include signal-to-noise ratio (snr) information. Furthermore, arrival times from global catalogs can have varied quality. For many arrival times reported to the USGS catalogs of the Chinese Digital Station Network (CDSN), travel times can have round-off or truncated reported times (Steck et al., 2000). Thus, for consistency and for handling the uncertainty of the travel-time picks, we assign measurement errors for regional P- and S-waves to be 1.0 s and 2.0 s, respectively. For the global catalog times, we assign the measurement errors for P- and S-waves to be 2.0 s and 3.0 s, respectively.

Modeling error is the error associated with the inadequacy of the velocity models to account for earth structure and affects the error ellipse estimation. For 1-D velocity models, the modeling error can be parameterized as a function of radial distance. We use the regional models from previous studies and the modeling errors that we developed for
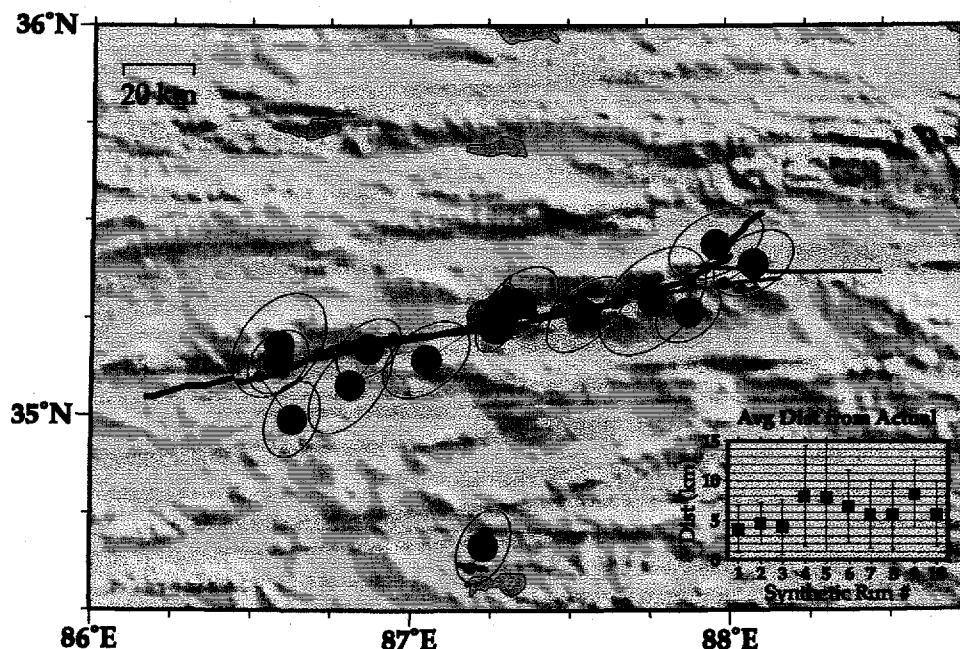
Figure 2. Relocations and 90% error ellipses for synthetic data. Data generated for select events around and including the main Manyi event on 08NOV1997. Selected events were placed on the main and secondary ruptures (black dots) to generate synthetic arrival data with added gaussian noise. This was done to test how well events could be constrained on the ruptures given normal arrival pick errors, with the velocity model known. Depth fixed at 33 km. Inset: Average distance from actual synthetic origin for ten synthetic location runs.

those models using teleseismic locations (Jih, 1998; Li and Mooney, 1998; Steck *et al.*, 2000). We also calculate travel times for *S* phases for these same 1-D velocity models, and add a Tibetan model (Jih, 1998).

This region of the world has some of the most dramatic crustal structure in the world, making 1-D velocity models particularly inadequate. Furthermore, for seismic events in the regional context, the number of observing stations is small and the signal-to-noise ratios (SNRs) of seismic phases can be low, contributing to location errors. Therefore, we also employ 2-D travel time corrections (or propagation path corrections - PPCs) based on residuals for regional 1-D velocity models that were developed using a kriging interpolation algorithm (Schultz *et al.*, 1998; Steck *et al.*, 2000). The advantage of using the kriging algorithm is that travel-time corrections and modeling error can both be estimated. The use of these 2-D travel time corrections removes the 20 km location bias observed for the Tibet mainshock event (Steck *et al.*, 2000).

Synthetic Tests and Relocation Procedure

The location algorithm is based on a Geiger method implemented using the EvLoc algorithm (Bratt and Bache, 1988; Nagy, 1996). The method has been modified to include 2-D kriged travel-time correction surfaces (Schultz *et al.*, 1998). To assess whether we have adequate azimuthal station coverage to obtain precise locations on the fault, we perform a suite of synthetic tests using the station and phase information that we have for the aftershocks. We select several events of various magnitudes and place them on the main and secondary ruptures to generate synthetic arrival data. Using our measurement error criteria as discussed above, we perform inversions to check that we obtain the synthetic locations. We then add gaussian noise (dependent on estimated pick and model error) to the picks, and perform the relocations. We perform this set of inversions ten times, with each run generating gaussian noise for the picks (Figure 2). This was done to test how well events could be constrained on the ruptures given normal arrival pick errors, with the velocity model known.

To assess the lateral resolution that we are obtaining, we fix the depth. We calculate the average mislocation for the suite of synthetic relocations to be ~5 km. Thus, given any noise in our data sets, we can expect that at best to be within 5 km of the actual epicenter. This number of course will vary per event. Furthermore, we discover that our error ellipse estimates appear to be slightly low, as two of the ten events lie outside of the 90% error ellipse. Thus,
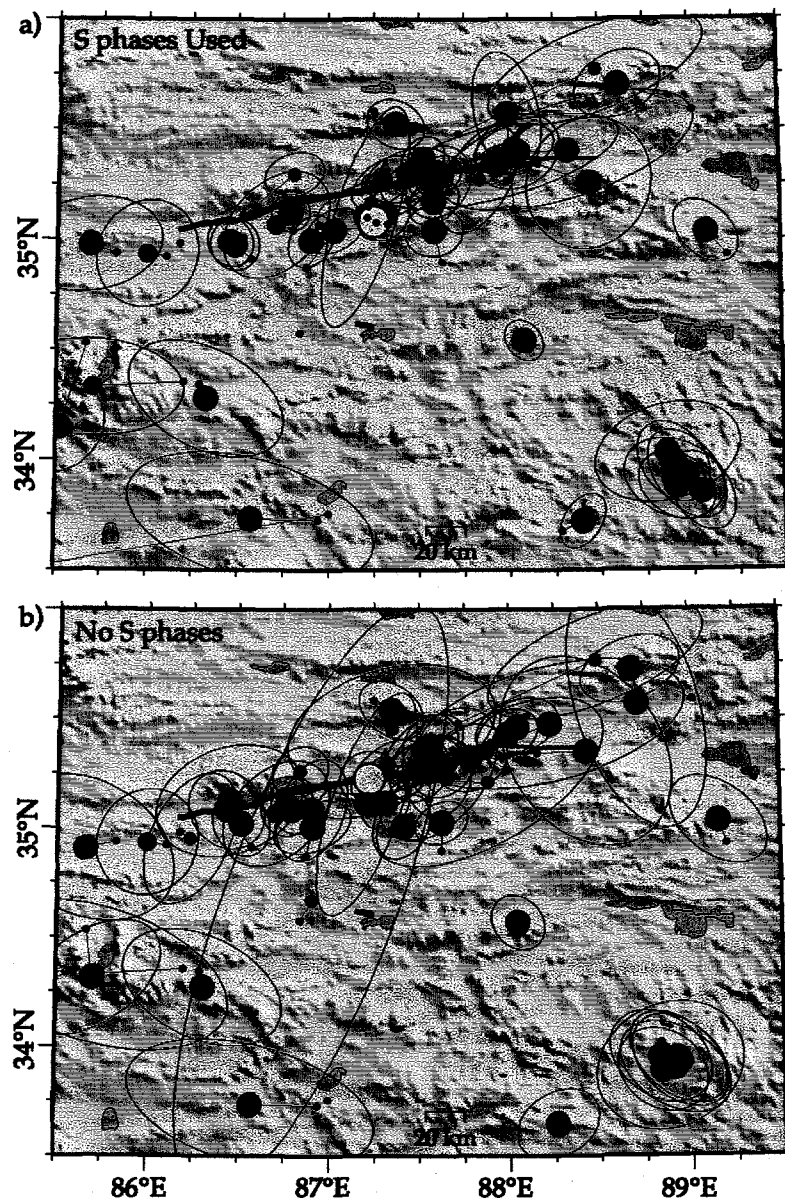
Figure 3. Relocations and error ellipses for EDR catalog locations around the 08NOV 1997 Tibet mainshock only for those events which had S phases. 2-D travel time corrections were used. Catalog locations are shown as black dots. a) S phases included in the relocation. Using S phases in the relocations does not correct for the southern bias in the mainshock (yellow). Several events were not relocated due to residual restrictions. b) Relocations without including S phases. The mainshock relocates to the trace of the main rupture.

we find that for events in the region, we should be able to obtain locations within 5 km of the fault given adequate data, and that we are slightly underestimating the error ellipses.

We attempted to include S phases as a means of improving the relocations for all the events shown in Figure 1 which had *S-wave* picks (Figure 3). PPCs were used for P phases in the locations. When including the S phases, many of the events could not be relocated due to residual restrictions (Figure 3a). Also, the mainshock location displays the southern bias observed in the catalog location. When S phases are excluded (Figure 3b), the mainshock is located on the main surface rupture. The location bias observed when including the S phases is not surprising given that there are no PPCs currently calculated for the S-wave models. Thus, we decided not to use S phases for relocating any of the secondary rupture candidate events.

Search for Secondary Rupture Event

As the first step in determining the candidate events for the secondary rupture, we determined which of the events from the EDR catalog were within the time period for the InSAR satellite pass and after the mainshock (08 NOV1997 - 02 DEC 1997) (Peltzer *et al.*, 1999). Of the events located near the main and secondary ruptures, 42 were possible candidates for the secondary rupture (Figure 1).

We placed the 42 candidate events on the secondary rupture, fixed the location and depth (3 km), and relocated using the IASP91 velocity model. The resulting values for the standard error for one observation (SDOBS) were analyzed to find the minimum values. Those events with low SDOBS values would become the best candidates for the secondary rupture. We chose a value of 3.0 s for SDOBS as a first cut for the 42 candidate events, leaving 11 events for further analysis.

Of the 11 events above, we determined which had the lowest average residuals. We limited this analysis to only regional stations with 2-D travel time correction surfaces. We calculated which events had the greatest percentage of phase residuals below 4.0 s, since the events all have differing number of defining phases. Any events with less than five regional defining stations before relocation and less than 50% of phases with absolute residuals below 4.0 s were discarded. We also tried to limit the remaining events to those with a relatively large percentage of manually repicked phases, leaving six candidate events. We further limited the remaining candidate events by discarding events that were obviously at too great a distance to be associated with the secondary rupture, which left three events (Figure 1).

We estimated the size of the event that caused the secondary rupture to be between M_w = 4.8-5.1, using the equation for moment magnitude (Lay and Wallace, 1995). The secondary rupture is ~5 km in length and has a displacement measured at least 0.1 m. The magnitude range was determined using a range of rupture depths from 1-5 km. After analyzing the waveforms of the three candidate events, we were able to discard one event based on the low SNR of the first arrivals at relatively near stations (MAKZ and LSA).

In order to investigate the two remaining candidate events (Figure 1), we analyzed waveforms for the first P arrivals and the Rayleigh waves for station MAKZ (Figure 4). The P arrivals display a similarity suggesting a common mechanism. We filtered the waveforms between 15 and 30 s to analyze the Rayleigh waves. Offset in the Rayleigh waves suggests a separation of ~29 km between the two events, relative to station MAKZ. The catalog locations display this approximate relative separation as should any relocations.

Relocation Results

The relocations for the two remaining candidate events are shown in Figure 3. We relocated the events using three different global and regional velocity models (IASP91, SSB (Jih, 1998), and TIBET (Jih, 1998)), PPCs when available (the TIBET model does not have calculated PPC surfaces), and a depth fixed at 3 km. To show relative relocation differences between the candidate events, we restricted the stations used in the relocation to those common to both events.

The relocations appear to migrate towards the main rupture surface instead of the secondary rupture surface. The SSB model actually shifted the 19 NOV1997 event to the main rupture surface trace. The above suggests that both candidate events were, most likely, located on or near the main rupture. The 90% error ellipses for the relocations also do not encompass any part of the secondary rupture. The relative distances between the relocated events are consistent with the ~29 km separation indicated by the Rayleigh wave offset. This again suggests that the candidate events are not associated with the secondary rupture.

We also relocated the candidate event above that was discarded due to lower than desired SNR at nearby stations. Using regional stations only with PPCs, the event relocated from ~106 km to ~28 km from the secondary rupture, the only event to relocate in relative proximity to the secondary rupture. However, when limiting the stations used to those common for the two candidate events above, the event relocated off the view of Figure 3, with one velocity model relocating the event far east, and the other two models relocating the event far west. Although this event did relocate near the secondary rupture, its instability precludes us from identifying it as the secondary rupture event. The lack of any candidate events to relocate close to the secondary rupture suggests that the secondary rupture was aseismic in nature or, most likely, coseismic with the mainshock event.
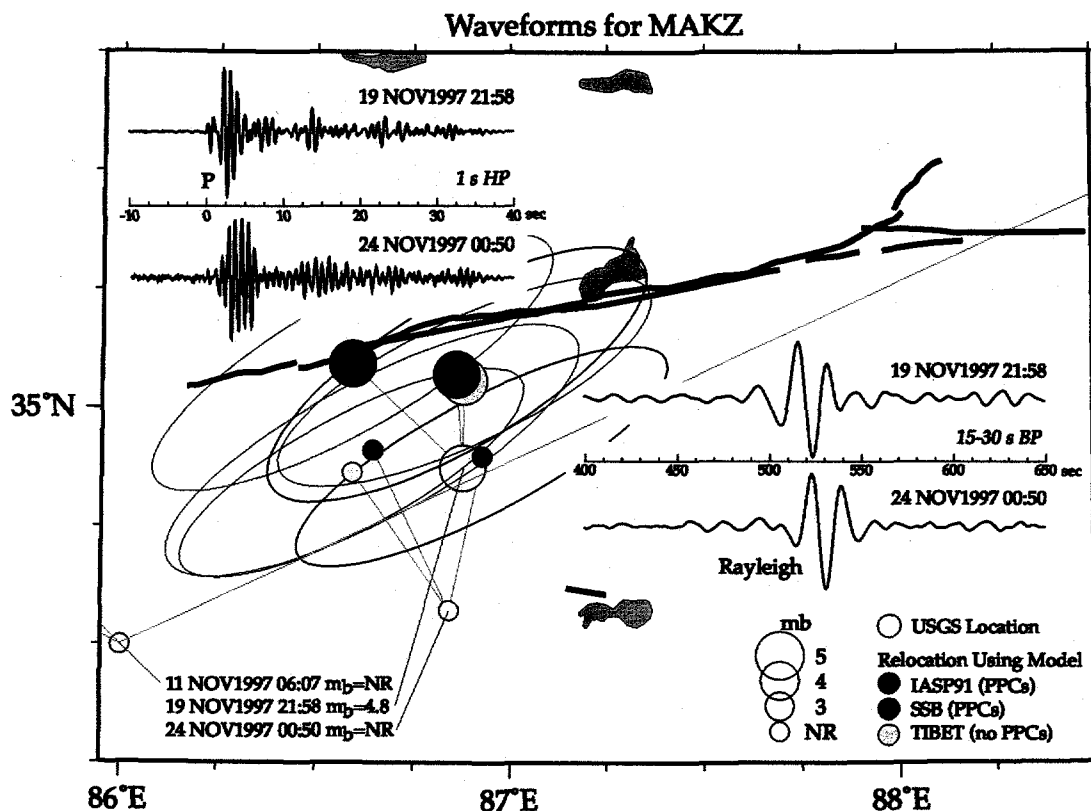
Waveforms for MAKZ

Figure 4. Catalog locations, relocations, and 90% confidence ellipses for two possible secondary rupture events. Both occurred during the appropriate time window (08NOV1997-02DEC1997). Relocations were determined using propagation path corrections (PPCs) when available and only those stations common to both events (i.e., ASAR, CMAR, FINES, GERES, HYB, LSA, MAKZ, SHL, WRA). IASP91 (red), SSB (green) (Jih, 1998), and TIBET (blue) (Jih, 1998) velocity models were used for the relocations. A third candidate event (lower left) was discarded due to low signal-to-noise ratio and relocation instability. Waveforms are shown for station MAKZ around the P (top left, 1 sec high-pass filter, time-aligned on P arrival) and Rayleigh arrivals (right, 15-30 sec band-pass filter, absolute time). The P-waves display a similarity suggesting a common mechanism. The offset in the Rayleigh waves indicates a separation of ~29 km between the two events, relative to station MAKZ. The relocated epicenters display this approximate separation. This suggests that neither event is related to the secondary rupture.

CONCLUSIONS AND RECOMMENDATIONS

InSAR can be a valuable tool for ground truth tests of event locations, particularly for those associated with CTBT studies. InSAR has already been successfully used as a ground truth test for the relocation of the Tibet mainshock using 2-D travel time corrections, removing the 20 km location bias (Steck *et al.*, 2000). We were able to limit the possible secondary rupture events by using synthetic tests with events restricted to the rupture trace identified by InSAR. InSAR also provides a means of estimating magnitude by providing information on fault displacement and area. Using this information, we were able to estimate the magnitude for a secondary rupture event at $M_w = 4.8$-5.1 which should have been detected by stations within regional distances. Analysis of the travel time residuals and the relocation results suggests that no cataloged event can be associated with the secondary rupture. Thus, the secondary rupture was aseismic in nature or, most likely, coseismic with the mainshock.

REFERENCES

Bratt, S. R., and T. C. Bache (1988). Locating events with a sparse network of regional arrays, *Bull. Seism. Soc. Am.* 78, 780-798.

Dewey, J. W. (1983). Relocation of instrumentally recorded pre-1974 earthquakes in the South Carolina region, in *Studies related to the Charleston, South Carolina, earthquake of 1886*, G. S. Gohn (Editor), *U. S. Geological Survey Professional Paper 1313*, Q1-Q9.

Jih, R.-S. (1998). Location calibration efforts in China, in *Proc. of the 20th Annual Seismic Research Symposium*, , 12.

Lay, T., and T. C. Wallace (1995). *Modern global seismology*, Academic Press, San Diego, California, 521 pp.

Li, S., and W. D. Mooney (1998). Crustal structure of China from deep seismic sounding profiles, in *Proc. of the 7th international symposium on Deep seismic profiling of the continents, Tectonophysics 288,* 105-113.

Molnar, P., and W.-P. Chen (1983). Focal depth and fault plane solutions of earthquakes under the Tibetan Plateau, *J. Geophys. Res.* 88, 1180-1196.

Myers, S. C., and C. A. Schultz (2000). Improving sparse network seismic location with bayesian kriging and teleseismically constrained calibration events, *Bull. Seism. Soc. Am.* 90, 199-211.

Nagy, W. (1996). New region-dependent travel-time handling facilities at the IDC: Functionality, testing, and implementation details, *SAIC Tech Rep. 96/1179*, 57 pp.

Peltzer, G., F. Crampé, and G. King (1999). Evidence of nonlinear elasticity of the crust from the Mw7.6 Manyi (Tibet) earthquake, *Science* 286, 272-276.

Schultz, C. A., S. C. Myers, J. Hipp, and C. J. Young (1998). Nonstationary Bayesian kriging; a predictive technique to generate spatial corrections for seismic detection, location, and identification, *Bull. Seism. Soc. Am.* 88, 1275-1288.

Steck, L. K., A. A. Velasco, A. H. Cogbill, and H. J. Patton (2000). Improving regional seismic event location in China, *Pure & Appl. Geophys.* in press.

Tapponnier, P., and P. Molnar (1977). Active faulting and tectonics in China, *J. Geophys. Res.* 82, 2905-2930.

Velasco, A. A., C. J. Ammon, and S. L. Beck (2000). Broadband source modeling of the November 8, 1997 Tibet (Mw = 7.5) earthquake and its tectonic implications, *J. Geophys. Res.* in press.